Axion Haloscope Array With $\mathcal{PT}$ Symmetry

Yifan Chen

ITP-CAS

based on arxiv 2103.12085

Y.C. , Minyuan Jiang, Yiqiu Ma, Jing Shu, Yuting Yang,

26 August 2021,
SUSY 2021, Beijing

Outlines

Motivation and Introduction to Axion

Axion/Axion-like Particle

- A hypothetical pseudoscalar originally motivated by the strong CP problem:
  Neutron electric dipole $|\bar{\theta}| 10^{-16}$ **e.cm is smaller than** 10^{-26} **e.cm.**

$$\bar{\theta} = \theta_{\mathrm{QCD}} + \arg \det M_u M_d, \qquad \text{Fine tuning!}$$

  Why is $\bar{\theta}$ so small? Why 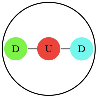

instead of 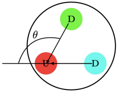

?
  Solution: introducing an **dynamical** field with effective potential

$$V \sim -m_\Phi^2 f_\Phi^2 \cos(\bar{\theta} + \frac{\Phi}{f_\Phi}).$$

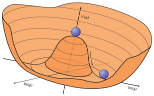

- Extra dimension predicts a wide range of axion mass.
  Dimensional reduction from higher form fields:
  e.g. $A^M(5D) \to A^\mu(4D) + \Phi(4D)$.

- Cold dark matter candidate.
  Coherent wave dark matter, very different from WIMP.

Oscillating Ultralight Scalar Background

- Non-relativistic light bosons behave as **coherent wave** when the occupation number is large:

$$\Phi(\vec{x}, t) \simeq \Phi_0(\vec{x}) \cos \omega_\Phi t; \qquad \Phi_0 \sim \frac{\sqrt{\rho_\Phi}}{m_\Phi}; \qquad \omega_\Phi \simeq m_\Phi .$$

- Cold dark matter candidate, wave-like when $m_\Phi < 1$ eV.
- **Oscillating field value** $\rightarrow$ **oscillating physical observables**:
  Dilaton: coupling constant, mass...
  Axion: EDM, chiral dispersion of photon...
- **The interactions with SM are suppressed by high scale.**
- **Amplifications of the signals:**
  Tabletop experiments on earth: $\rho_{\rm DM} \sim 0.4~\mathrm{GeV/cm^3}$;
  Astrophysical: **larger** ρ_Φ, e.g., galaxy center or near Kerr black hole.

Electromagnetic Resonant Detection

of Axion Dark Matter

Axion QED: Inverse Primakoff Effect

- Axion-electrodynamics modifies Maxwell equations:

$$\nabla \cdot \mathbf{E} = \rho - g_{\Phi\gamma}\mathbf{B} \cdot \nabla\Phi$$
$$\nabla \times \mathbf{B} = \partial_t \mathbf{E} + \mathbf{J} - g_{\Phi\gamma}\left(\mathbf{E} \times \nabla\Phi - \mathbf{B}\partial_t\Phi\right)$$

- Neglecting spatial derivative, background $\mathbf{B}_0$ and **axion dark matter** Φ leads to **effective current**

$$J_{\rm eff}(t) \sim g_{\Phi\gamma} B_0(t)\sqrt{\rho_{\rm DM}}\cos m_\Phi t.$$

- Inverse Primakoff effect: the conversion of axion to an **oscillating EM field** under background $\mathbf{B}_0$.

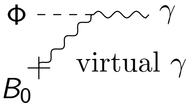

Resonant Cavity with static B_0 [P.Sikivie 83']

- Cavity mode equation:

$$\sum_n \left(\partial_t^2 + \frac{\omega_n}{Q_n}\partial_t + \omega_n^2 \right) \mathbf{E}_n = g_{\Phi\gamma}\partial_t \left(\mathbf{B}_0 \partial_t \Phi \right)$$

- Traditional setup with static B_0:

$$\partial_t \mathbf{B}_0 = 0, \quad \omega_1 = m_\Phi;$$

- Scanning the axion mass by tunning ω_1 is difficult since $\omega \sim V^{-1/3}$, only within one order around GHz.

e.g. ADMX, HAYSTACK

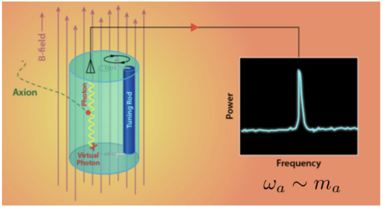

Resonant LC circuit [P.Sikivie et al 14']

- Scanning the mass $m_\Phi = \omega_{\rm LC} = \frac{1}{\sqrt{LC}}$ from 100 Hz to 100 MHz by **tuning the capacitor C**.

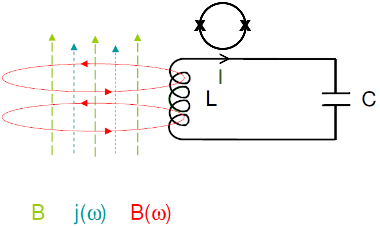

DM Radio science: axions

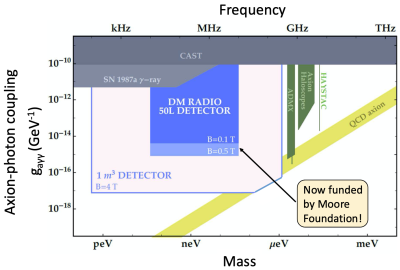

Assumptions: T=10 mK, Q=10^6, 3.5 year integration time, quantum-limited readout

e.g. DM radio, ADMX-SLIC

Resonant SRF Cavity with AC B_0 [A.Berlin, R.T. D'Agnolo, et al 19']

$$\sum_n \left(\partial_t^2 + \frac{\omega_n}{Q_n}\partial_t + \omega_n^2\right) \mathbf{E}_n = g_{\Phi\gamma}\partial_t \left(\mathbf{B}_0 \partial_t \Phi\right).$$

- Using an AC pump mode of B_0:

$$\partial_t \mathbf{B}_0 = i\omega_0 \mathbf{B}_0, \quad \omega_1 - \omega_0 = m_\Phi;$$

- Scanning the mass by **tuning the differences between two quasi-degenerate and transverse modes**.

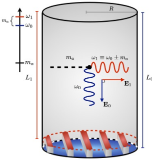

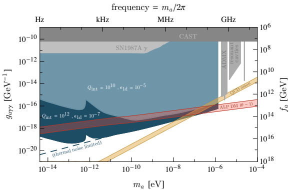

- High $Q_{\rm int} > 10^{10}$ due to the superconducting nature.

Quantum noise limit for resonant detection

- **Standard quantum limit for power law detection**: [Chaudhuri, Irwin, Graham, Mardon 18']

  resonant intrinsic noise $S_{\rm int}$ + flat readout noise $S_{\rm r}$.

- Sensitivity to $S_{\rm sig}$ and $S_{\rm int}$ is the same.

  SNR^2 $\propto$ range where $S_{\rm int} \gg S_{\rm r}$.

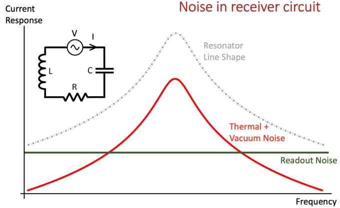

- **Beyond quantum limit**:

  Squeezing $S_{\rm r}$, e.g., HAYSTACK.

  Increasing the sensitivity to $S_{\rm sig}$, e.g., white light cavity in optomechanics [Miao, Ma, Zhao, Chen 15'].

Axion Haloscope Array With $\mathcal{PT}$ Symmetry

White Light Cavity [X.Li, M.Goryachev, Y.Ma et al 20']

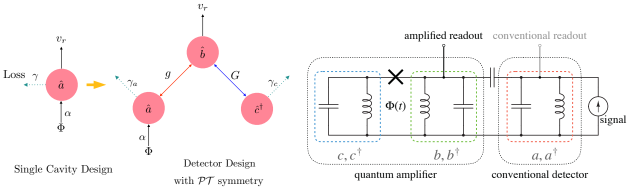

- **Beam-splitting**: $\hbar g(\hat{a}\hat{b}^\dagger + \hat{a}^\dagger\hat{b})$.
- **Non-degenerate parametric amplifier**: $\hbar G(\hat{b}\hat{c} + \hat{b}^\dagger\hat{c}^\dagger)$.

- $\mathcal{PT}$**-symmetry** $(\hat{a} \leftrightarrow \hat{c}^\dagger)$ **emerges** when $g = G$.

$$\begin{aligned}(\dot{\hat{a}} + \dot{\hat{c}}^\dagger) &= -i(g-g)\hat{b} - i\alpha\Phi + \cdots ; \\ \dot{\hat{b}} &= -\gamma_r\hat{b} - ig(\hat{a} + \hat{c}^\dagger) + \cdots .\end{aligned}$$

- Coherent cancellation leads to **double resonance**. $S_{\rm sig}$ is largely enhanced when $g \gg$ **intrinsic dissipation** γ:

$$S^{\rm WLC}_{\rm sig}(\Omega) = \frac{2\gamma_r\alpha^2 S_\Phi(\Omega)}{(\gamma+\gamma_r)^2 + \Omega^2}\left(\frac{g^2}{\gamma^2+\Omega^2}\right).$$

Resonator Chain Haloscope

- Generalization to chain detector:

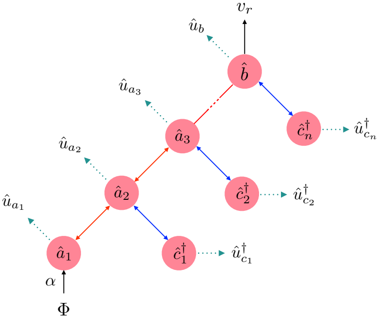

- $\mathcal{PT}$-invariant mode: $\hat{A}_i \equiv \hat{a}_i + \hat{c}_i^\dagger$.

$$\dot{\hat{A}}_1 = -i\alpha\Phi + \cdots\,,$$
$$\dot{\hat{A}}_i = -ig\hat{A}_{i-1} + \cdots\,,$$
$$\dot{\hat{b}} = -\gamma_r\hat{b} - ig\hat{A}_n.$$

$n+1$-times resonance!

- The whole Hamiltonian is explitly $\mathcal{PT}$ **broken**.

- $S_{\rm sig}$ is n-times enhanced:

$$S_{\rm sig}^{\rm RC}(\Omega) = \frac{2\gamma_r\alpha^2 S_\Phi(\Omega)}{(\gamma+\gamma_r)^2+\Omega^2}\left(\frac{g^2}{\gamma^2+\Omega^2}\right)^n.$$

Binary Tree Haloscope

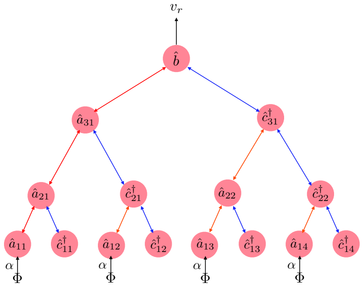

- **Fully $\mathcal{PT}$-symmetric setup** with $\hat{a}_{ij} \leftrightarrow \hat{c}^\dagger_{ij}$ as well as all the modes below.

- Signal PSD has additional coherent enhancement $\propto 2^{2n-2}$ due to the multi probing sensors:

$$S_{\rm sig}^{\rm BT}(\Omega) = \frac{\gamma_r \alpha^2 S_\Phi(\Omega)}{2((\gamma+\gamma_r)^2+\Omega^2)} \left(\frac{4g^2}{\gamma^2+\Omega^2}\right)^n.$$

Signal to Noise Ratio

- **SNR^2 $\propto$ range where $S_{\mathbf{int}} \gg S_{\mathbf{r}}$** increases with n:

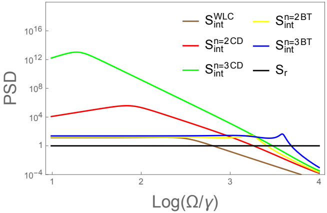

- In binary tree, SNR is additionally enhanced by $\sim 2^n$ due to the uncorrelation of the noise modes:

$$\mathrm{SNR} \simeq 2^{n-1} \left(\frac{g}{\gamma n_{\mathrm{occ}}} \right)^{\frac{n}{2n+1}} \frac{\rho_{\mathrm{DM}} \alpha^2}{m_\Phi^3} \sqrt{\frac{Q_\Phi t_e}{\gamma n_{\mathrm{occ}}}}.$$

- g/γ **can be as large as** $Q_{\mathbf{int}}$.

Robustness Analysis

- $\mathcal{PT}$-breakings when $g \neq G$ or $\gamma_a \neq \gamma_c$:

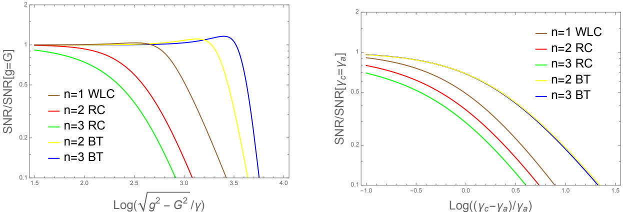

- **Binary tree is more robust than the resonator chain** due to the approximate $\mathcal{PT}$ symmetry.

- **Larger n increases the robustness** due to the enhanced general $\mathcal{PT}$ group.

Physics Reach

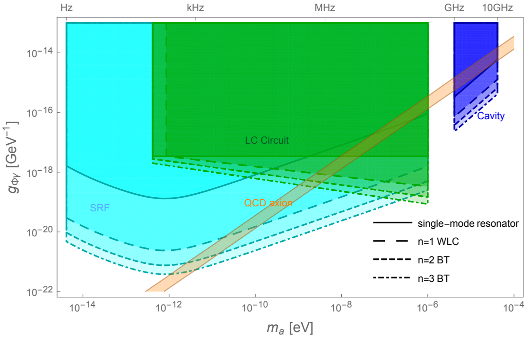

- The large thermal noise at low frequency for LC circuit makes the enhancement ineffective.

- Due to the high quality factor, **BT based on SRF** can cover most of the QCD axion dark matter phase space potentially.

Summary and Prospect

- **Multi modes of resonator** can go far beyond the quantum limit from the readout noise.
- The SRF haloscope, with **a high quality factor**, can probe most of the QCD axion mass window.
- **Quantum metrology** can play huge rules in fundamental physics!

Thank you

Appendix

Axion Coupling to the Standard Model

- **Axion Fermion coupling**: $\partial_\mu \Phi \bar{\psi} \gamma^\mu \gamma_5 \psi / f_\Phi$,
  non-linearization of a chiral global symmetry $\sim \partial_\mu \Phi J_5^\mu / f_\Phi$.
  Stellar cooling, DM wind/gradient.

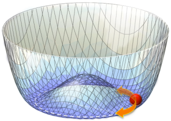

- **Axion Gluon coupling**: $\Phi \mathrm{Tr}\, G_{\mu\nu} \tilde{G}^{\mu\nu} / f_\Phi$,
  generated from anomaly/triangle loop diagram.
  Oscillating EDM.

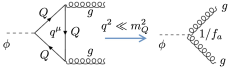

- **Axion Photon coupling**: $\Phi F_{\mu\nu} \tilde{F}^{\mu\nu} / f_\Phi$,
  from mixing with neutral π_0.
  Photon conversion to axion, inverse Primakoff, birefringence.

Misalignment Production of QCD Axion

- For QCD axion, $m_\Phi f_\Phi \sim \Lambda^2_{\mathrm{QCD}}$ predicts a **thin line in the parameter space**.
- Cosmological parameter: initial misalignment angle $\theta_i \equiv \Phi_i / f_\Phi$.

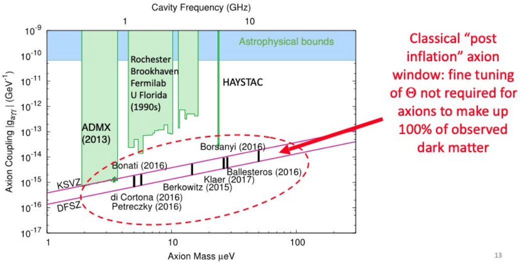

- Assuming $\theta_i \sim 1$ leads to the most natural region of QCD axion dark matter $m_\Phi \sim 10^{-6}\mathrm{eV} \sim$ GHz.
- Different cosmological evolutions can still provide a viable dark matter candidate in other region, e.g., PQ symmetry broken before inflation.

Property of Axion Dark Matter

Galaxy formation: virialization gave $\sim 10^{-3}c$ velocity fluctuation, thus kinetic energy $\sim 10^{-6} m_\Phi c^2$ currently.

Effectively coherent wave:

$$\Phi(\vec{x}, t) = \frac{\sqrt{2\rho_\Phi}}{m_\Phi} \cos\left(\omega_\Phi t - \vec{k}_\Phi \cdot \vec{x} + \delta_0\right).$$

- Bandwidth: $\delta\omega_\Phi \simeq m_\Phi \left\langle v_{\mathrm{DM}}^2 \right\rangle \simeq 10^{-6} m_\Phi,\ Q_\Phi \simeq 10^6$.
- Correlation time: $\tau_\Phi \simeq \mathrm{ms}\,\frac{10^{-6}\mathrm{eV}}{m_\Phi}$.
  Power law detection is used to make integration time longer than τ_Φ.
- Correlation length: $\lambda_d \simeq 200\ \mathrm{m}\frac{10^{-6}\mathrm{eV}}{m_\Phi} \gg \lambda_c = 1/m_\Phi$.
  Sensor array can be used within λ_d.

Higher Frequency Electromagnetic Resonant Detection

Difficult to detect $m_\Phi \gg$ GHz axion dark matter due to short λ_c.

I 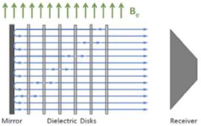

II 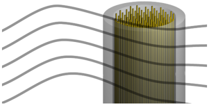

III 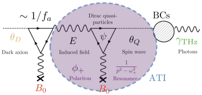

- I **Dielectric Haloscope**: discontinuity of E-field leads to coherent emission of photons from each surface, up to 50 GHz. [A.Caldwell et al 17']
- II **Plasma Haloscope**: using tunable cryogenic plasma to match axion mass, up to 100 GHz. [M.Lawson et al 19']
- III **Topological Insulator**: quasiparticle in it mixing with E field becomes polariton whose frequency can be tuned by magnetic field, up to THz. [D.J.E.Marsh et al 19']

Quantization of Cavity/Circuit Mode

- In Coulomb gauge, vector potential can be quantized

$$\vec{A}_k(\vec{r},t) = \sum_k \left(\frac{1}{2\omega_k}\right)^{1/2} \hat{a}_k u_k(\vec{r}) e^{-i\omega_k t} + h.c..$$

where $u_k(\vec{r})$ form a complete orthonormal set for a given boundary condition and $[\hat{a}_k, \hat{a}_{k'}] = \delta_{kk'}$.

- The Hamiltonian for each mode reduces to harmonic oscillator

$$H_{\rm cavity} = \frac{1}{2}\int \left(\vec{E}^2 + \vec{B}^2\right) d^3\vec{x} = \sum_k \omega_k \left(\hat{a}_k^\dagger \hat{a}_k + \frac{1}{2}\right).$$

- In the interaction picture, the coupling to axion is

$$H_{\rm int} = \int g_{\Phi\gamma} \Phi \vec{E} \cdot \vec{B}_0 d^3\vec{x} = \alpha\Phi(\hat{a} + \hat{a}^\dagger), \quad \alpha \simeq g_{\Phi\gamma} B_0 \sqrt{m_\Phi V}.$$

- Circuit mode can be quantized in the same way

$$H_{\rm LC} = \frac{\hat{Q}^2}{2C} + \frac{\hat{\phi}^2}{2L} = \omega_{\rm LC}\left(\hat{a}^\dagger \hat{a} + \frac{1}{2}\right).$$

Open quantum system

A quantum-mechanical system interacting with the environment:

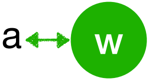

- System mode $\hat{a}$ couples to infinite degrees of freedom $\hat{w}_\omega$:

$$i\hbar\sqrt{2\gamma_r}\int_{-\infty}^{+\infty}\frac{d\omega}{2\pi}[\hat{a}^\dagger\hat{w}_\omega - \hat{a}\hat{w}_\omega^\dagger] + \int_{-\infty}^{+\infty}\frac{d\omega}{2\pi}\hbar\omega\hat{w}_\omega^\dagger\hat{w}_\omega.$$

- Fourier transformation: **0-dim localized mode** $\hat{a}$ couples to an 1-dim bulk w_ξ (transmission line):

$$i\hbar\sqrt{2\gamma_r}\hat{a}^\dagger\hat{w}_{\xi=0} + \mathrm{h.c.} + i\hbar\int_{-\infty}^{+\infty} d\xi\,\hat{w}_\xi^\dagger\partial_\xi\hat{w}_\xi.$$

- Equations of motion for $\hat{a}$ and outgoing mode $\hat{w}_{0_+}$:

$$\dot{\hat{a}} = -\gamma_r\hat{a} + \sqrt{2\gamma_r}\hat{w}_{0_-}; \qquad \hat{w}_{0_+} = \hat{w}_{0_-} - \sqrt{2\gamma_r}\hat{a}$$

Single Mode Resonator as Quantum Sensor

- For a resonator $\hat{a}$ **probing weak signal** Φ: $\alpha\left(\hat{a}+\hat{a}^{\dagger}\right)\Phi$
- Readout for outgoing mode $\hat{v}_r \equiv \hat{w}_{0_+}$:

$$\hat{v}_r = \frac{\Omega - i\gamma_r}{\Omega + i\gamma_r}\hat{u}_r + \frac{\sqrt{2\gamma_r}\alpha}{\Omega + i\gamma_r}\Phi.$$

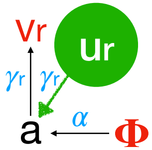

- Vacuum fluctuation in incoming mode $\hat{u}_r \equiv \hat{w}_{0_-}$ with white noise power spectral density $S_{\mathrm{r}} = 1$.
- Resonant signal spectrum $S_{\mathrm{sig}} = \frac{2\gamma_r\alpha^2}{\gamma_r^2+\Omega^2}\ S_\Phi(\Omega)$.

$$\text{Scan rate: } \int_{-\infty}^{+\infty} \frac{2\gamma_r\alpha^2}{\gamma_r^2+\Omega^2}d\Omega = \frac{\alpha^2}{2\pi}.$$

- Trade-off between peak sensitivity and bandwidth by tuning γ_r.

Intrinsic loss and fluctuation

- However, **intrinsic loss** proportional to γ exists, characterized by the quality factor $Q_{\rm int} \equiv \omega/\gamma$.

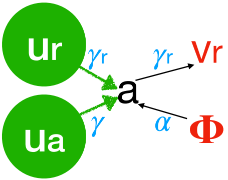

- According to the **fluctuation-dissipation theorem**, there is intrinsic noise $S_{\rm int}(\Omega) = \frac{4\gamma\gamma_r}{(\gamma+\gamma_r)^2+\Omega^2} S_{u_a}$ whose PSD contains both vacuum and thermal fluctuations:

$$S_{u_a} = n_{\rm occ} \equiv \left(\frac{1}{2} + \frac{1}{\exp(\omega/T) - 1}\right) \simeq \begin{cases} \frac{1}{2} & T \ll \omega; \\ \frac{T}{\omega} & T \gg \omega. \end{cases}$$

- **Standard quantum limit for power law detection:** **resonant** $S_{\rm int}$ + **flat** $S_{\rm r}$. [Chaudhuri et al 18']

Beam splitting coupling

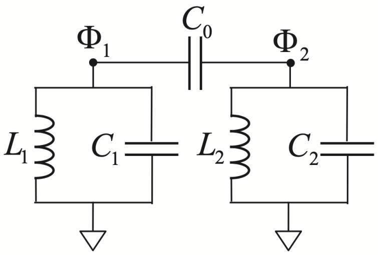

- Use an additional capacitor to couple two LC circuits:

$$H = \frac{1}{2}C_1\dot{\phi}_1^2 + \frac{1}{2}C_2\dot{\phi}_2^2 + \frac{1}{2L_1}\phi_1^2 + \frac{1}{2L_2}\phi_2^2 + \frac{1}{2}C_0(\dot{\phi}_1 - \dot{\phi}_2)^2.$$

- Conjugate momentum to ϕ_i involves mixing. Interaction potential:

$$\beta\hbar\sqrt{\omega_1\omega_2}(\hat{a}_1 - \hat{a}_1^\dagger)(\hat{a}_2 - \hat{a}_2^\dagger) \sim \hat{a}_1\hat{a}_2^\dagger + h.c.,$$

Non-Degenerate Parametric amplifier coupling

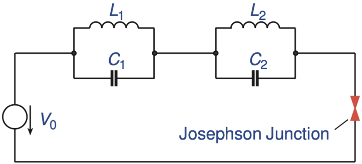

- Use a DC voltage and a Josephson junction to couple two LC circuits:

$$
\begin{aligned}
V &= -\frac{\hbar I_J}{2e_0}\cos\left(\omega_0 t + \frac{2e_0}{\hbar}(\phi_2+\phi_3)\right) \\
&= -\frac{\hbar I_J}{2e_0}\cos\left(\omega_0 t + \kappa_2(a_2+a_2^\dagger) + \kappa_3(a_3+a_3^\dagger)\right) \\
&\sim \frac{\hbar I_J}{4e_0}\kappa_2\kappa_3[a_2a_3 + a_2^\dagger a_3^\dagger],
\end{aligned}
$$

Kinetic Mixing Dark Photon Dark Matter

- An additional $U(1)$ vector can have kinetic mixing with electromagnetic photon field through
$$\varepsilon F_{\mu\nu} F'^{\mu\nu}.$$
- It appears generally in theory with extra-dimension with a broad mass window predicted.
- Cold dark matter candidate behaving like **coherent wave**:

From Axion QED to Kinetic Mixing Dark Photon

$$\nabla \times \mathbf{B} = \partial_t \mathbf{E} + \mathbf{J} - g_{\Phi\gamma} \left(\mathbf{E} \times \nabla\Phi - \mathbf{B}\partial_t\Phi \right)$$

- Axion dark matter leads to an effective current under background $\mathbf{B}_0$ with $|J_{\rm eff}(t)| \sim g_{\Phi\gamma} B_0(t) \sqrt{\rho_{\rm DM}} \cos m_\Phi t$.

$$-\frac{1}{4}\left(\tilde{F}_{\mu\nu}\tilde{F}^{\mu\nu} + \tilde{F}'_{\mu\nu}\tilde{F}'^{\mu\nu}\right) + \frac{1}{2} m_{\gamma'}^2 \tilde{A}'_\mu \tilde{A}'^\mu - e J^\mu_{\rm EM} \tilde{A}_\mu + \varepsilon m_{\gamma'}^2 \tilde{A}_\mu \tilde{A}'^\mu.$$

- Similarly, in the interaction basis, the background dark photon behaves as an effective electromagnetic current with $J^\mu_{\rm eff} = \varepsilon m_{\gamma'}^2 \tilde{A}'^\mu$.

Effective current induced magnetic field

- In a space screened by electromagnetic shielding, the effective current can induce a transverse magnetic field

- For axion:

$$\begin{aligned} B_a &\approx |\vec{J}_a^{\text{eff}}| \, V^{1/3}, \\ &\approx 10^{-17}\mathrm{T} \left(\frac{g_{a\gamma}}{10^{-11}\ \mathrm{GeV}^{-1}} \right) \left(\frac{B_0}{1\ \mathrm{T}} \right) \left(\frac{V^{1/3}}{1\ \mathrm{m}} \right) \end{aligned}$$

- For kinetic mixing dark photon (with a factor of 1/3 due to the isotropic wave-funtion):

$$\begin{aligned} B_{dp} &\approx |\vec{J}_{dp}^{\text{eff}}| \, V^{1/3}, \\ &\approx 10^{-16}\mathrm{T} \left(\frac{\varepsilon}{10^{-6}} \right) \left(\frac{m_{dp}}{10\mathrm{Hz}} \right) \left(\frac{V^{1/3}}{1\ \mathrm{m}} \right). \end{aligned}$$

- V is the volume of the EM shielding room. Magnetic field signal is the strongest at the corner of the room.